

Quantum lattice-gas model of spinor superfluids

Jeffrey Yepez¹, George Vahala², Linda Vahala³, Min Soe⁴

¹ *Air Force Research Laboratory, Hanscom Air Force Base,*

Massachusetts 01731 ²*Department of Physics, William & Mary, Williamsburg, Virginia 23185*

³*Department of Electrical & Computer Engineering, Old Dominion University, Norfolk, VA 23529*

⁴*Department of Mathematics and Physical Sciences, Rogers State University, Claremore, OK 74017*

Keywords: quantum lattice gas, quantum computation, spinor superfluid, coupled BECs, Skyrmions

ABSTRACT

Spinor Bose Einstein Condensates are intriguing because of their vast range of different topological vortices. These states occur when a BEC gas is trapped in an optical lattice rather than in a magnetic well (which would result in scalar BEC vortices). A spinor BEC states also occur in a quantum gas when several hyperfine states of the atom co-exist in the same trap. A unitary quantum lattice algorithm that is ideally parallelized to all available processors is used to solve the evolution of non-eigenstate Skyrmions in a coupled BEC system. The incompressible kinetic energy spectrum of the inner quantum vortex ring core rapidly deviates from the k^{-3} spectrum found in the evolution of scalar BECs.

INTRODUCTION

A quantum lattice gas model is presented as an ab initio representation of spinor superfluid dynamics. The quantum lattice-gas representation constitutes a quantum computing algorithm useful for modeling spinor superflows comprising two Bose-Einstein condensates (BECs). A thorough review of spinor BECs has recently been provided by Ueda and Kawaguchi [3]. The lowest order effective field theory describing the long-wavelength behavior of the interacting condensate fields, φ_+ and φ_- , are the coupled Gross-Pitaevskii (GP) equations

$$i\partial_t\varphi_+ = -\nabla^2\varphi_+ - \frac{\mu^2}{2}\varphi_+ + \frac{\lambda^2}{2}|\varphi_+|^2\varphi_+ + \frac{\lambda^2}{2}|\varphi_-|^2\varphi_+ + \dots \quad (1a)$$

$$i\partial_t\varphi_- = -\nabla^2\varphi_- - \frac{\mu^2}{2}\varphi_- + \frac{\lambda^2}{2}|\varphi_+|^2\varphi_- + \frac{\lambda^2}{2}|\varphi_-|^2\varphi_- + \dots, \quad (1b)$$

where μ and λ are real-valued coupling constants. The coupled GP equations can be written as

$$i\partial_t\varphi_+ = -\nabla^2\varphi_+ + \frac{\mu^2}{2}\left(\frac{\lambda^2}{\mu^2}\rho - 1\right)\varphi_+ \quad (2a)$$

$$i\partial_t\varphi_- = -\nabla^2\varphi_- + \frac{\mu^2}{2}\left(\frac{\lambda^2}{\mu^2}\rho - 1\right)\varphi_-, \quad (2b)$$

where the total number density is $\rho \equiv |\varphi_+|^2 + |\varphi_-|^2 = \rho_+ + \rho_-$. With the 2-component field $\Phi \equiv \begin{pmatrix} \varphi_+ \\ \varphi_- \end{pmatrix}$, the equation of motion for the coupled like-component BEC system is simply

$$i\partial_t\Phi = -\nabla^2\Phi + a(gp - 1)\Phi, \quad (3)$$

where the spacetime scale factor is $a \equiv \frac{\mu^2}{2}$ and the coupling energy is $g \equiv \frac{\lambda^2}{\mu^2}$. The quantum algorithm is a straightforward generalization of that already tested for the single-component BEC case [4, 5]. Yet, in the multiple-component model, we can now explore new phenomena such as line defects in the phase of the respective condensates that are topologically linked. Along the topological defect the magnitude of the condensate field vanishes. Thus a defect is identified by the zero of the condensate field. The linked defect that we study here is a quantum vortex line (in spinor component 2) along the z -axis threading through the center of a small vortex ring (in spinor component 1) in the xy -plane. The quantum vortex line along the z -axis in condensate 2 is of finite length and self-connected is at each of its ends by a toroidal surface of zero density, so that technically it is only a vortex line within the interior of the vortex ring in condensate 2. This type of two-component condensate soliton comprising linked topological defects is known as a Skyrmion.

SKYRMIONS

A Skyrmion is a 3-sphere in \mathbb{R}^4 of radius R : $\sum_{n=1}^4 x_n^2 = R^2$. A point on the 3-sphere is specified with three spherical angles. Let us denote the two elevation angles by $0 < \alpha \leq \pi$ and $0 < \beta \leq \pi$, and the azimuthal angle by $0 < \gamma \leq 2\pi$. That is, a point, with coordinates (w, x, y, z) , on the 3-sphere in the spherical angles is:

$$w = \sin \alpha \sin \beta \cos \gamma \quad (4a)$$

$$x = \sin \alpha \sin \beta \sin \gamma \quad (4b)$$

$$y = \sin \alpha \cos \beta \quad (4c)$$

$$z = \cos \alpha. \quad (4d)$$

Using complex representation with real and imaginary components and a 2-spinor field with upper and lower components, the four coordinates in (4) can be faithfully represented as

$$\Phi \equiv \begin{pmatrix} z - iy \\ x - iw \end{pmatrix} = \begin{pmatrix} \cos \alpha - i \sin \alpha \cos \beta \\ -i \sin \beta \sin \alpha e^{i\gamma} \end{pmatrix}. \quad (5)$$

To obtain a 3D Skyrmion, we can embed the 3-sphere into \mathbb{R}^3 with the following map:

$$\pi \tanh(kr) \equiv \alpha(r, \vartheta, \phi) \quad \vartheta \equiv \beta(r, \vartheta, \phi) \quad \phi \equiv \gamma(r, \vartheta, \phi), \quad (6)$$

where r , ϑ , and ϕ are the spherical coordinates in \mathbb{R}^3 . The parameter k in (6) is positive and real-valued and it is a spatial scaling factor that determines the size of the 3D Skyrmion. Notice the first elevation angle in \mathbb{R}^4 is mapped into the radial direction in \mathbb{R}^3 so that the Skyrmion Φ field fills space.

Let us consider a system of Skyrmions in a box of size L^3 with the n th Skyrmion being located at position $\mathbf{x}_n \equiv (x_n, y_n, z_n)$. We denote the radial distance from the center of the Skyrmion at \mathbf{x}_n to the field observation point $\mathbf{x} \equiv (x, y, z)$ as

$$r_n(x, y, z) \equiv |\mathbf{x} - \mathbf{x}_n| = \sqrt{(x - x_n)^2 + (y - y_n)^2 + (z - z_n)^2}. \quad (7)$$

The n th Skyrmion 2-spinor field is

$$\Phi_n(\mathbf{x}) = \begin{pmatrix} \cos [\pi \tanh(kr_n)] - i \sin [\pi \tanh(kr_n)] \frac{z - z_n}{r_n} \\ -i \left(1 - \frac{(z - z_n)^2}{r_n^2}\right)^{\frac{1}{2}} \sin [\pi \tanh(kr_n)] e^{i\phi_n} \end{pmatrix}, \quad (8)$$

where $\phi_n \equiv \arctan\left(\frac{y - y_n}{x - x_n}\right)$ and where to ensure that the Skyrmion is contained within the box we consider a parameter regime where $kL \gg 1$. In this limit, there is a well defined background field in the box

$$\Phi_{n0}(\mathbf{x}) = \begin{pmatrix} \varphi_{n+} \\ \varphi_{n-} \end{pmatrix}_o = \begin{pmatrix} -1 \\ 0 \end{pmatrix}, \quad (9)$$

for a single Skyrmion. The probability fields of a single Skyrmion $\Phi = \begin{pmatrix} \varphi_+ \\ \varphi_- \end{pmatrix}$ are shown in Fig. 1, indicating the Skyrmion is topologically equivalent to a Hopf link - a two linked quantum vortices. It is interesting to note that the isosurfaces of the component BEC densities $\rho_+ \equiv |\varphi_+|^2$ and $\rho_- \equiv |\varphi_-|^2$ switch roles: for vortex core isosurface $|\varphi_+|^2 = |\varphi_-|^2 = 0.1$, the condensate wavefunction φ_+ is the inner ring vortex while the condensate wavefunction φ_- is the linear vortex core through the ring vortex and which closes on the outer surface to resemble an apple core. However for isosurfaces $|\varphi_+|^2 = |\varphi_-|^2 = 0.1$, φ_+ is the outer isosurface while φ_- is the inner ring isosurface. The Skyrmion is a coreless topological defect because at the nodal line where the first condensate vanishes, $\varphi_+ = 0$, the second condensate is a maximum, $\varphi_- = 1$, and vice versa. So, along a nodal line in a spinor BEC $\rho = 1$. For unity coupling $g = 1$, the last term on the right-hand side of (3) vanishes along the nodal lines. This is the opposite behavior of a single component BEC where along a defect line $\rho = 0$.

In the far field limit for the n th Skyrmion, $|\mathbf{x} - \mathbf{x}_n| \gg 1$, $\varphi_{n+}(\mathbf{x}) \rightarrow -1$ and $\varphi_{n-}(\mathbf{x}) \rightarrow 0$. Hence to create multiple Skyrmions (whose centers are initially well separated in space) for a single composite 2-spinor field, one may simply multiply the top spinor components and add the bottom spinor components as follows:

$$\Phi(\mathbf{x}) = \bigotimes_{n=1}^N \Phi_n(\mathbf{x}) = \begin{pmatrix} \prod_{n=1}^N \varphi_{n+}(\mathbf{x}) \\ \sum_{n=1}^N \varphi_{n-}(\mathbf{x}) \end{pmatrix}. \quad (10)$$

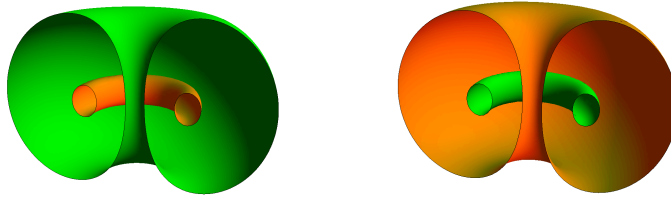


FIG. 1: Isosurfaces of $|\varphi_+|^2 = |\varphi_-|^2 = 0.1$ (left) and $|\varphi_+|^2 = |\varphi_-|^2 = 0.9$ (right) for a single Skyrmion sliced in half to see the inner quantum vortex ring. The condensates switch roles: for isosurfaces = 0.1 the inner quantum vortex core of the φ_+ condensate while the quantum vortex along the z -axis is associated with φ_- and resembles an apple core as the top of the linear vortex bends around to connect to the bottom.

Hence, there is a well defined background value of the composite field

$$\Phi_o(\mathbf{x}) = \begin{pmatrix} (-1)^N \\ 0 \end{pmatrix} \quad (11)$$

for the N Skyrmons.

Quadrupole

If the net spin of a configuration of a set of Skyrmons has zero net angular momentum, then the simplest initial conditions one may consider is two oppositely charged Skyrmons, a particle-antiparticle pair. Furthermore, if periodic boundary conditions are imposed on the embedding space, then the simplest configuration one may consider is a quadrupole configuration of Skyrmons (a pair of particle-antiparticle pairs). That is, the simplest topology is a **quadrupolar configuration**, comprising four Skyrmons, that has zero net angular momentum and that may be placed in a box with periodic boundary conditions. Letting a plus sign ($\circ+$) denote a Skyrmion oriented normal to the plane of the paper, with one unit of positive circulation 2π and letting a minus sign ($\circ-$) denote one unit of negative circulation -2π , then an example quadrupolar configuration (4 Skyrmons) is

$$\begin{array}{cc} \circ- & \circ+ \\ & \\ \circ+ & \circ- \end{array} \quad (12)$$

An example for $N = 4$ (four Skyrmons in the $z = 0$ plane of a box of size $L = 1024$) with Φ_1 located at $\mathbf{x}_1 = (\frac{L}{4}, \frac{L}{4}, \frac{L}{2})$, Φ_2 located at $\mathbf{x}_2 = (\frac{L}{4}, \frac{3L}{4}, \frac{L}{2})$, Φ_3 located at $\mathbf{x}_3 = (\frac{3L}{4}, \frac{L}{4}, \frac{L}{2})$, and Φ_4 located at $\mathbf{x}_4 = (\frac{3L}{4}, \frac{3L}{4}, \frac{L}{2})$ is

$$\Phi^{\text{quad}}(\mathbf{x}) \equiv \Phi_1(\mathbf{x}) \otimes \Phi_2(\mathbf{x}) \otimes \Phi_3(\mathbf{x}) \otimes \Phi_4(\mathbf{x}) = \left(\frac{\prod_{n=1}^4 \varphi_{n+}(\mathbf{x})}{\sum_{n=1}^4 \varphi_{n-}(\mathbf{x})} \right). \quad (13)$$

Its composite probability fields are rendered in Fig. 2. With the center of the quadrupole at $\mathbf{x}_o = (x_o, y_o, z_o)$, the positions of the Skyrmion centers may be written as

$$\mathbf{x}_1 = (x_o - \delta, y_o - \delta, z_o) \quad (14a)$$

$$\mathbf{x}_2 = (x_o - \delta, y_o + \delta, z_o) \quad (14b)$$

$$\mathbf{x}_3 = (x_o + \delta, y_o - \delta, z_o) \quad (14c)$$

$$\mathbf{x}_4 = (x_o + \delta, y_o + \delta, z_o). \quad (14d)$$

So Fig. 2 shows the quadrupole with $\mathbf{x}_o = (\frac{L}{2}, \frac{L}{2}, \frac{L}{2})$ and $\delta = \frac{L}{4}$. The radial distances from the Skyrmion lines (parallel to the z -axis) are

$$\begin{array}{ll} r_1(x, y) = (x - x_o - \delta)^2 + (y - y_o - \delta)^2 & r_2(x, y) = (x - x_o - \delta)^2 + (y - y_o + \delta)^2 \\ r_3(x, y) = (x - x_o + \delta)^2 + (y - y_o - \delta)^2 & r_4(x, y) = (x - x_o + \delta)^2 + (y - y_o + \delta)^2. \end{array} \quad (15)$$

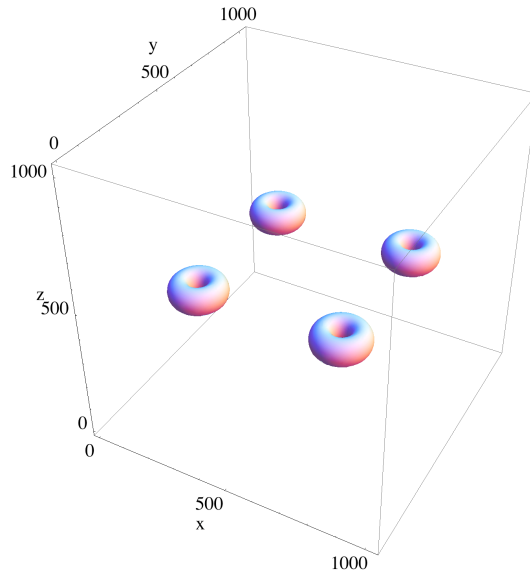


FIG. 2: Four Skyrmions in a box of size $L = 1024$ with $k = 10/L$ rendered with a probability isosurface threshold of 0.5. The background composite spinor field is $\Phi_o = (1, 0)$. For probability isosurface of 0.5, the two composite BEC condensates φ_+ and φ_- isosurfaces coincide.

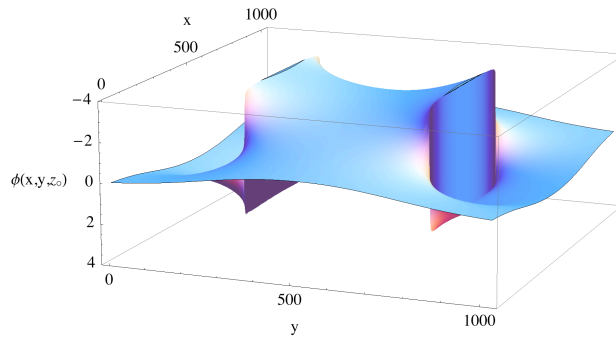


FIG. 3: A slice at $z = z_o$ of the magnitude phase contours of the wave function for a Skyrmion quadrupole, the product of $N = 4$ Skyrmions centered in a box of size $L = 1024$. From the phase diagram, plotted $-\pi \lesssim \phi(x, y, z_o) \lesssim \pi$, going around any contour in the $z = z_o$ plane (that encloses a single Skyrmion singularity) accumulates a phase of $\pm 2\pi$ radians. With four Skyrmions one can accommodate periodic boundary conditions in the phase.

The size of the Skyrmion quadrupole is $|\delta|$, its overall center is (x_o, y_o, z_o) , and we define its **polarity** to be $\text{sign}(\delta) = \pm 1$. The phase angles are

$$\begin{aligned}
 \phi_1(x, y) &= \arctan \frac{y - y_o - \delta}{x - x_o - \delta} & \phi_2(x, y) &= \arctan \frac{y - y_o - \delta}{x - x_o + \delta} \\
 \phi_3(x, y) &= \arctan \frac{y - y_o + \delta}{x - x_o - \delta} & \phi_4(x, y) &= \arctan \frac{y - y_o + \delta}{x - x_o + \delta}.
 \end{aligned} \tag{16}$$

The phase of (13) is plotted in Fig. 3 with $\delta = \frac{L}{4}$ for $L = 1024$, demonstrating the periodicity of the quadrupolar configuration. We shall use such quadrupole configurations (aligned along an orthogonal principal lattice direction, say) to represent initial conditions for numerical simulations.

QUANTUM SIMULATION

Two simulations are presented. First, we consider the time evolution of a single Skyrmion initial condition which, because of some rescaling, is not an eigenstate of the time-independent rescaled coupled GP equation. Moreover

since there is only a single Skyrmion initial condition, there is a net angular momentum in the system. We will then consider the interaction of four Skyrmions in which there is no net angular momentum.

Unitary Quantum Lattice Gas Algorithm

We now briefly describe our unitary quantum lattice gas algorithm to solve the spinor BEC equations. The simplest algorithm is a straightforward extension of the algorithm for a scalar BEC. To recover the scalar GP equation for the component φ_+ , we introduce 2 qubits on each lattice site, $|\psi\rangle = |q_1 q_2\rangle$. Considering the 1-body sector, let α denote the amplitude associated with the 2-qubit state $|01\rangle$, and let β denote the amplitude with the 2-qubit state $|10\rangle$. Thus at each site \mathbf{x} on a cubic lattice

$$\psi(\mathbf{x}, t) = \begin{pmatrix} \alpha(\mathbf{x}, t) \\ \beta(\mathbf{x}, t) \end{pmatrix}. \quad (17)$$

At each lattice site \mathbf{x} , these excited state probability amplitudes are entangled by a local unitary collision operator of the form

$$C = e^{i\frac{\pi}{4}\sigma_x(1-\sigma_x)}, \quad (18)$$

where the σ are the Pauli spin matrices

$$\sigma_x = \begin{pmatrix} 0 & 1 \\ 1 & 0 \end{pmatrix} \quad \sigma_y = \begin{pmatrix} 0 & -i \\ i & 0 \end{pmatrix} \quad \sigma_z = \begin{pmatrix} 1 & 0 \\ 0 & -1 \end{pmatrix}. \quad (19)$$

The local qubit entanglement is then propagated throughout the lattice by streaming operators

$$S_{\Delta\mathbf{x},0} = n + e^{\Delta\mathbf{x}\partial_x} \bar{n}, \quad S_{\Delta\mathbf{x},1} = \bar{n} + e^{\Delta\mathbf{x}\partial_x} n, \quad (20)$$

where $n = \frac{1}{2}(1 - \sigma_z)$ and $\bar{n} = \frac{1}{2}(1 + \sigma_z)$. unitarily shift the components of ψ along $\pm\Delta\mathbf{x}$, respectively. In essence, (20) unitarily shifts just one of these post-collision excited state amplitude probability to the nearest neighbor lattice site $\mathbf{x} \pm \Delta\mathbf{x}$, respectively. In particular, let us first consider the evolution operator for the γ th component of ψ . Our quantum algorithm interleaves the noncommuting collide and stream operators, *i.e.* $[S_{\Delta\mathbf{x},\gamma}, C] \neq 0$,

$$I_{x\gamma} = S_{-\Delta\mathbf{x},\gamma} C S_{\Delta\mathbf{x},\gamma} C \quad (21)$$

where γ is either 0 or 1 corresponding to the streaming of either the α or β component of ψ in (17). Since $|\Delta\mathbf{x}|$ is small the interleaved sequence $I_{x\gamma}^2$, (21), is close to unity since $C^4 = 1$, the identity operator.

Consider the following evolution operator for the γ component of φ_+

$$U_\gamma[\Omega(\mathbf{x})] = I_{x\gamma}^2 I_{y\gamma}^2 I_{z\gamma}^2 e^{-i\varepsilon^2\Omega(\mathbf{x})}, \quad (22)$$

where we introduce a small perturbation parameter ε in the exponent and Ω will be specified later. With this evolution operator, the time advancement of the state ψ is given by

$$\psi(\mathbf{x}, t + \Delta t) = U_\gamma[\Omega] \psi(\mathbf{x}, t). \quad (23)$$

After considerable algebra, it can be shown that for the particular unitary collide-stream operators in (18) and (20), one obtains the following quantum lattice gas equation on expanding in the perturbation parameter ε

$$\begin{aligned} \psi(\mathbf{x}, t + \Delta t) &= \psi(\mathbf{x}, t) - i\varepsilon^2 \left[-\frac{1}{2}\sigma_x \nabla^2 + \Omega \right] \psi(\mathbf{x}, t) \\ &\quad + \frac{(-1)^\gamma \varepsilon^3}{4} (\sigma_y + \sigma_z) \nabla^3 \psi(\mathbf{x}, t) + \mathcal{O}(\varepsilon^4), \end{aligned} \quad (24)$$

with $\gamma = 0$ or 1. Since the order ε^3 term in (24) changes sign with γ , one can eliminate this term by introducing the symmetrized evolution operator

$$U[\Omega] = U_1 \left[\frac{\Omega}{2} \right] U_0 \left[\frac{\Omega}{2} \right]. \quad (25)$$

rather than U_γ .

Under diffusion ordering, in the scaling limit $[\psi(\mathbf{x}, t + \Delta t) - \psi(\mathbf{x}, t)] \rightarrow \varepsilon^2 \partial_t \psi(\mathbf{x}, t)$, the quantum map

$$\psi(\mathbf{x}, t + \Delta t) = U[\Omega(\mathbf{x})] \psi(\mathbf{x}, t) \quad (26)$$

leads to a representation of the two-component parabolic equation

$$i\partial_t \psi = \left[-\frac{1}{2} \sigma_x \nabla^2 + \Omega \right] \psi(\mathbf{x}, t) + \mathcal{O}(\varepsilon^2), \quad (27)$$

where the operator Ω is still arbitrary. To recover the scalar GP equation, one simply rescales the spatial grid $\nabla \rightarrow a^{-1} \nabla$, contracts the 2-component field ψ to the (scalar) BEC wave function φ_+

$$\varphi_+ = (1, 1) \cdot \psi = \alpha + \beta \quad (28)$$

and chooses $\Omega = g|\varphi_+|^2 - 1$:

$$i\partial_t \varphi_+ = -\nabla^2 \varphi_+ + a(g|\varphi_+|^2 - 1)\varphi_+ + \mathcal{O}(\varepsilon^2). \quad (29)$$

To recover the spinor-GP system

$$i\partial_t \varphi_+ = -\nabla^2 \varphi_+ + a [g(|\varphi_+|^2 + |\varphi_-|^2) - 1] \varphi_+ + \mathcal{O}(\varepsilon^2). \quad (30)$$

$$i\partial_t \varphi_- = -\nabla^2 \varphi_- + a [g(|\varphi_+|^2 + |\varphi_-|^2) - 1] \varphi_- + \mathcal{O}(\varepsilon^2). \quad (31)$$

one simply introduces another 2-qubits $|\psi'\rangle = |q'_1 q'_2\rangle$ to represent the φ_- wave function and generalizes the operator Ω to

$$\Omega = g(|\varphi_+|^2 + |\varphi_-|^2) - 1. \quad (32)$$

Single Skyrmion

We first consider the evolution of a non-eigenstate single Skyrmion for the spinor superfluid given by

$$i\partial_t \Phi = -\nabla^2 \Phi + a(g\rho - 1)\Phi. \quad (33)$$

where the 2-component field $\Phi \equiv \begin{pmatrix} \varphi_+ \\ \varphi_- \end{pmatrix}$, and total number density is $\rho \equiv |\varphi_+|^2 + |\varphi_-|^2 = \rho_+ + \rho_-$. For these simulations, we choose $a=0.02$ and $g = 0.5$. In Fig. 4, the early time evolution of the isosurfaces $|\varphi_+|^2 = |\varphi_-|^2 = 0.0625$ (i.e., the vortex cores of the two condensates are shown). The outer apple core isosurface of φ_- has had its front surface culled so as to expose the dynamics of the inner quantum vortex ring of φ_+ . One sees the quantum vortex ring in the first component of the spinor condensate start with the filamentary topological defect $|\varphi_+| = 0$ (circular nodal line) and deforms over time into an areal topological defect (cupped nodal surface).

In Fig. 5, we show the kinetic energy spectrum of the first component of the Skyrmion for the quantum simulation shown in Fig. 4, i.e., the compressible and incompressible kinetic energies of the initial vortex ring isosurface core for φ_+ . The initial k^{-3} incompressible kinetic energy spectrum for the vortex ring is quickly destroyed. On the other hand, the incompressible kinetic energy spectrum for the apple-core isosurface (i.e., for condensate φ_-) remains around k^{-3} throughout the simulation run.

At late times, the single Skyrmion has grown to sufficient size to strongly interact with itself because of the periodic boundary conditions of the 1024^3 box, and the Skyrmion breaks apart. Remarkably, the spinor BEC forms a random lattice cycling through Skyrmion-like defect configurations. Fig. 6 shows an example of this random lattice of Skyrmion-like defects. The filling fraction of the first condensate is too low to support quantum vortex rings around all the available quantum vortex nodal lines in the lattice. Therefore, the first condensate randomly percolates through the lattice of the second condensate.

Four Skyrmion quadrupole

Fig. 7 show the time evolution of a four Skyrmions aligned in a quadrupolar configuration. Again, parameters chosen in the simulation runs are $a = 0.02$ and $g=0.5$ (33) are used and for early times the Skyrmions deform individually as in Fig. 4.

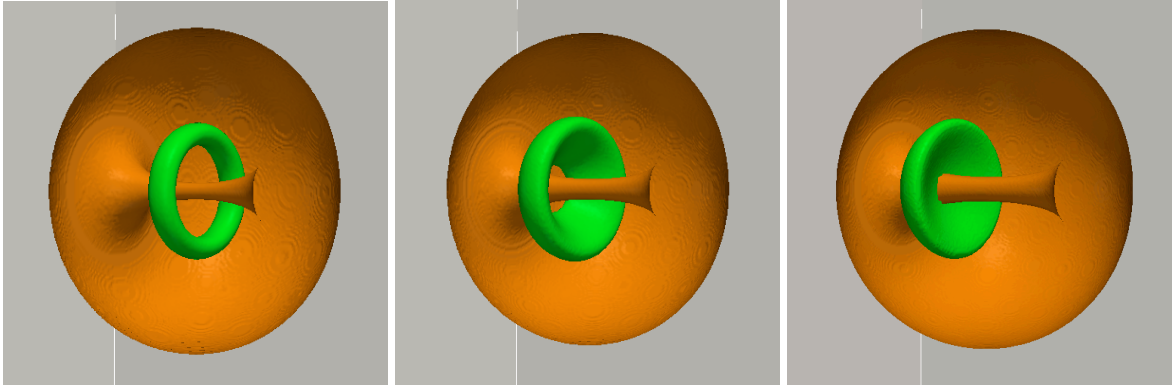


FIG. 4: Time development of a single Skyrmion at times $t = 0$, $t = 2000$, and $t = 4000$. The filamentary vortex ring deforms into an areal and cupped shaped nodal defect (green) while the linear vortex remains stable. At latter times the size of the Skyrmion steady increases (since it is not an eigenstate) until it reaches the boundary of the box of size $L = 1024$.

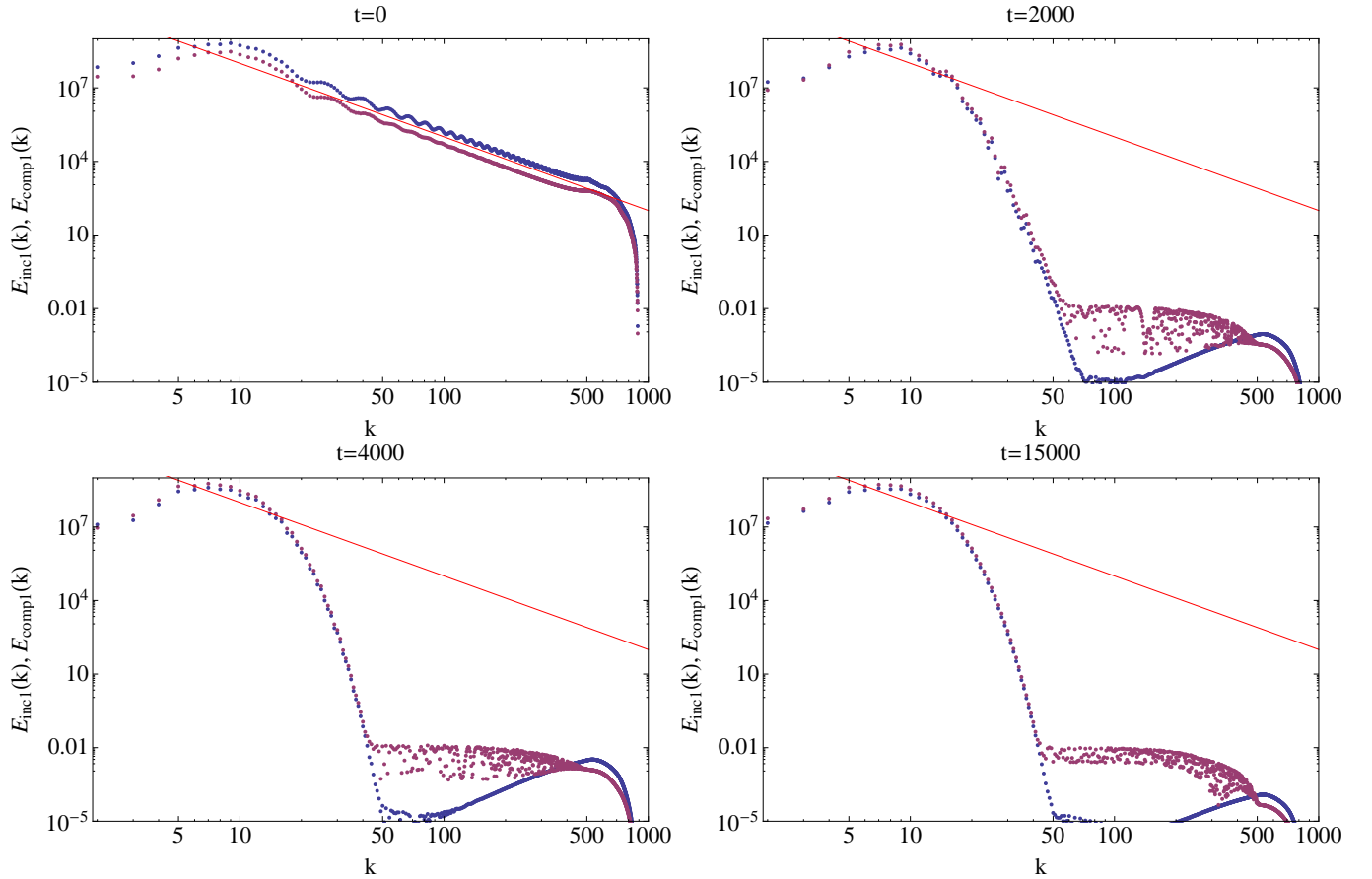


FIG. 5: The kinetic energy spectrum of the first component of the Skyrmion at times $t = 0$, $t = 2000$, $t = 4000$, and $t = 15000$. The red line is the theoretical spectrum for a filamentary quantum vortex, which is a k^{-3} power-law. At later times, the spectrum quickly departs from the k^{-3} line spectrum. The data points are the incompressible kinetic energy (red) and the compressible kinetic energy (blue).

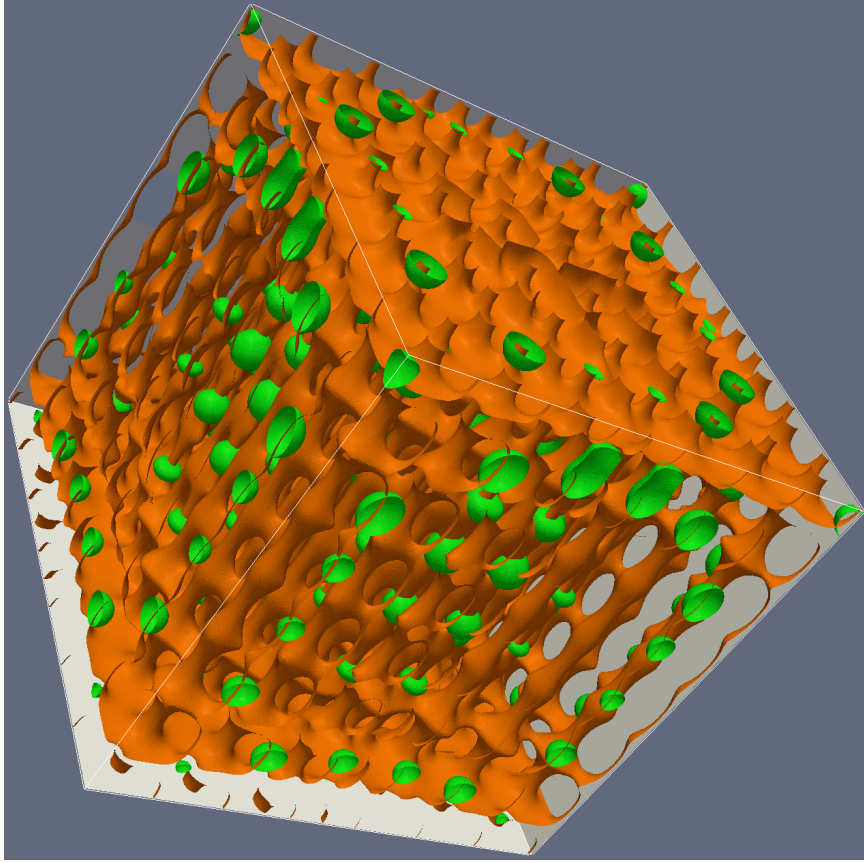


FIG. 6: Interaction of four Skyrmions at the late time $t = 235000$ leads to a random array of Skyrmion-like topological defects where the first condensate (green) continually percolates throughout a vortex lattice (orange) of the second condensate component.

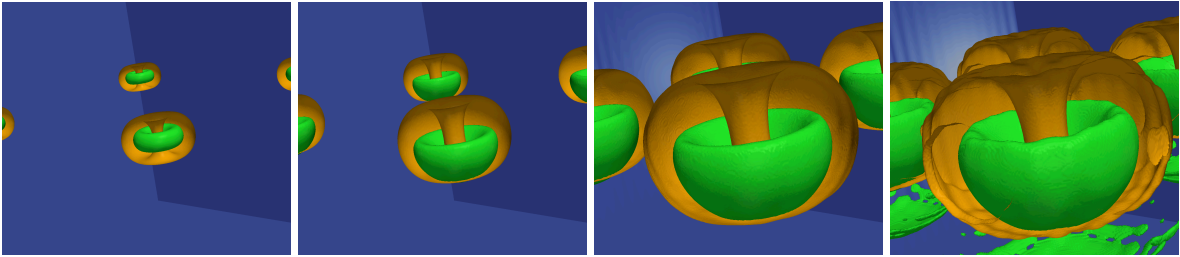


FIG. 7: Time development of a four Skyrmions at times $t = 0$, $t = 5000$, and $t = 15000$. The increase in the Skyrmion size as it reaches the boundary of the box of size $L = 1024$ is readily apparent.

CONCLUSION

We have extended our scalar BEC quantum lattice algorithm to be able to handle spinor BECs. In particular, we have shown simulation runs for the evolution of non-eigenstate Skyrmions. A spinor BEC can support far richer vortex structures than their scalar BEC counterpart. The scalar GP equation [1, 2] describes the evolution of a BEC gas trapped in a magnetic well with the spin of the atoms locked to the local magnetic field. This results in vortex topology governed by the Abelian group $U(1)$. However, if the BEC gas is in an optical trap, the spin orientation of the atoms can change dynamically resulting in spinor GP systems [3]. One can now find non-Abelian vortices. It remains an open question on how the non-Abelian vortices will affect quantum turbulence because of the topological constraints imposed on which vortices can interact with other vortices. These questions are currently under investigation.

- [1] Gross, E. P., 1963, *J.Math.Phys.* **4**(2), 195.
- [2] Pitaevskii, L. P., 1961, *Soviet Phys. JETP* **13**(2), 451.
- [3] Ueda, M., and Y. Kawaguchi, 2010, arXiv:cond-mat.quant-gas.1001.2072v2 (pages 7), URL <http://arxiv.org/abs/1001.2072>.
- [4] Yepez, J., G. Vahala, and L. Vahala, 2009, *Euro. Phys. J. Special Topics* **171**, 9.
- [5] Yepez, J., G. Vahala, L. Vahala, and M. Soe, 2009, *Physical Review Letters* **103**(8), 084501 (pages 4), URL <http://link.aps.org/abstract/PRL/v103/e084501>.